Available online at www.sciencedirect.com

SCIENCE DIRECT

Physics Letters B 636 (2006) 40–45

PHYSICS LETTERS B

www.elsevier.com/locate/physletb

On the re-summation of enhanced pomeron diagrams

S. Ostapchenko

Forschungszentrum Karlsruhe, Institut für Kernphysik, 76021 Karlsruhe, Germany
D.V. Skobeltsyn Institute of Nuclear Physics, Moscow State University, 119992 Moscow, Russia

Received 23 May 2005; received in revised form 15 February 2006; accepted 5 March 2006

Available online 20 March 2006

Editor: J.-P. Blaizot

Abstract

Dominant contributions of enhanced pomeron diagrams to elastic hadron–hadron scattering amplitude are re-summed to all orders. The formalism is applied to calculate total hadronic cross sections and elastic scattering slopes. An agreement with earlier results is obtained.

1. Introduction

Despite a significant progress in the perturbative QCD during last decades one still has to rely on phenomenological approaches when calculating total hadron–hadron cross sections, diffraction dissociation probabilities, or when treating particle production in general minimum bias hadronic collisions. The most powerful one proved to be the Gribov's reggeon approach [1], where high energy interactions are described as multiple scattering processes, elementary re-scatterings being treated phenomenologically as pomeron exchanges, as shown in Fig. 1.

Usual ansatz for the pomeron amplitude in impact parameter representation is [2]

$$f^{\mathbb{P}}_{ad}(s,b) = \frac{i\gamma_a\gamma_d (s/s_0)^{\alpha_{\mathbb{P}}(0)-1}}{\lambda_{ad}(s)} e^{-\frac{b^2}{4\lambda_{ad}(s)}}, \tag{1}$$

$$\lambda_{ad}(s) = R_a^2 + R_d^2 + \alpha'_{\mathbb{P}}(0)\ln(s/s_0), \tag{2}$$

where s and b are c.m. energy squared and impact parameter for the interaction, $s_0 \simeq 1$ GeV^2 is the hadronic mass scale, $\alpha_{\mathbb{P}}(0)$ and $\alpha'_{\mathbb{P}}(0)$ are the intercept and the slope of the pomeron Regge trajectory, and γ_a, R_a^2 are the coupling and the slope of pomeron–hadron a vertex.

Considering any number of pomerons exchanged between hadrons a and d one obtains elastic scattering amplitude as a sum of contributions of diagrams of Fig. 1 [2]:

$$\begin{aligned} i f_{ad}(s,b) &= \frac{1}{C_a C_d}\sum_{n=1}^{\infty}\frac{[iC_aC_d f^{\mathbb{P}}_{ad}(s,b)]^n}{n!} \\ &= \frac{1}{C_aC_d}\big[e^{-\chi^{\mathbb{P}}_{ad}(s,b)} - 1\big], \end{aligned} \tag{3}$$

$$\chi^{\mathbb{P}}_{ad}(s,b) = \frac{1}{i} C_a C_d f^{\mathbb{P}}_{ad}(s,b), \tag{4}$$

where shower enhancement coefficient C_a accounts for low mass inelastic intermediate states for hadron a; $\chi^{\mathbb{P}}_{ad}$ is the pomeron quasi-eikonal.

This allows one to calculate total cross section $\sigma^{\rm tot}_{ad}$ and elastic scattering slope $B^{\rm el}_{ad}$ as

$$\begin{aligned} \sigma^{\rm tot}_{ad}(s) &= 2\,{\rm Im}\int d^2b\, f_{ad}(s,b) \\ &= \frac{2}{C_aC_d}\int d^2b\big[1 - e^{-\chi^{\mathbb{P}}_{ad}(s,b)}\big], \end{aligned} \tag{5}$$

$$\begin{aligned} B^{\rm el}_{ad}(s) &= \frac{d}{dt}\ln\frac{d\sigma^{\rm el}_{ad}(s,t)}{dt}\bigg|_{t=0} \\ &= \frac{1}{C_aC_d\sigma^{\rm tot}_{ad}(s)}\int d^2b\, b^2\big[1 - e^{-\chi^{\mathbb{P}}_{ad}(s,b)}\big], \end{aligned} \tag{6}$$

where $d\sigma^{\rm el}_{ad}(s,t)/dt$ is the differential elastic cross section for momentum transfer squared t. Comparing to data one obtains typically $\alpha_{\mathbb{P}}(0) \simeq 1.1$, $\alpha'_{\mathbb{P}}(0) \simeq 0.2$ GeV^{-2} [3].

E-mail address: serguei.ostapchenko@ik.fzk.de (S. Ostapchenko).

0370-2693
doi:10.1016/j.physletb.2006.03.026

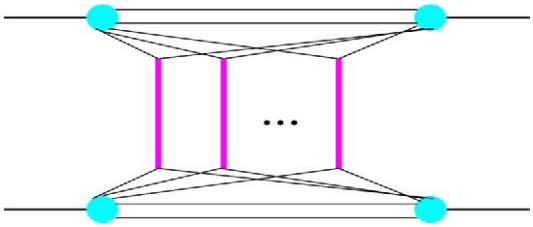

Fig. 1. General multi-pomeron contribution to hadron–hadron scattering amplitude; elementary scattering processes (vertical thick lines) are described as pomeron exchanges.

Making use of Abramovskii–Gribov–Kancheli cutting rules [4] allows one to re-sum contributions of various unitarity cuts of the elastic scattering diagrams of Fig. 1, corresponding to particular inelastic final states of hadron–hadron interactions. This opens the way for developing powerful model approaches [3] and for constructing Monte Carlo generators for hadronic and nuclear collisions [5].

Still, the underlying picture for the described scheme corresponds to an interaction mediated by a number of independent parton cascades. In "dense" regime, i.e. in the limit of high energies and small impact parameters, one expects a large number of such elementary scattering processes. Then, the underlying parton cascades should largely overlap and interact with each other, giving rise to significant non-linear effects [6]. The Latter are traditionally described by enhanced pomeron diagrams, which involve pomeron–pomeron interactions [7,8]. However, consistent treatment of enhanced corrections proved to be a very non-trivial problem: as the energy increases more and more diagrams of complicated topologies come into play.

General approach to the re-summation of higher order enhanced graphs has been proposed in [9] assuming π-meson dominance of multi-pomeron vertices. It has been shown that in the limit of very high energies the full pomeron scheme is equivalent to the above-described quasi-eikonal picture, however, based on a pomeron with suitably renormalized intercept. An alternative procedure was suggested in [10], where one resummed dominant enhanced corrections to hadron–nucleus and nucleus–nucleus scattering amplitudes postulating a negligibly small pomeron slope and including only triple-pomeron vertices. However, corresponding algorithms cannot be applied to treat general inelastic final states in hadronic interactions.

Present Letter is devoted to a direct all-order re-summation of enhanced contributions to hadron–hadron elastic scattering amplitude. The analysis of corresponding unitarity cuts and applications of the approach to particle production treatment are discussed elsewhere [11].

2. The formalism

Comparatively simple generalization of the previous scheme can be obtained using eikonal vertexes g_{mn} for the transition of m into n pomerons, $g_{mn} = r_{3\mathbb{P}}\gamma_{\mathbb{P}}^{m+n-3}/(4\pi m!n!)$, with $r_{3\mathbb{P}}$ being the triple-pomeron coupling. In particular, assuming pion dominance of multi-pomeron vertices, one has $g_{mn} = \frac{G}{C_\pi^2}(C_\pi\gamma_\pi)^{m+n}/m!/n!$ and the vertex slope $R_{\mathbb{P}}^2$ is equal to the

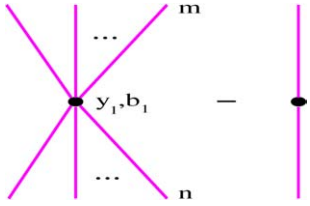

Fig. 2. Lowest order enhanced graphs; pomeron connections to the projectile and target hadrons not shown explicitely.

one of pomeron–pion coupling R_π^2 [8,9]. Thus, for a pomeron exchanged between two vertices one uses the quasi-eikonal for pion–pion scattering $\chi_{\pi\pi}^{\mathbb{P}}(s_0e^{\Delta y}, \Delta b)$, as defined by (4), (1), (2), where Δy and Δb are rapidity and impact parameter distances between the vertices. Correspondingly, a pomeron exchange between hadron a and a given vertex is described by $\chi_{a\pi}^{\mathbb{P}}(s_0e^{\Delta y}, \Delta b)$. This way the contribution with only one multi-pomeron vertex is obtained using standard reggeon calculus techniques [1,2]: summing over $m \geqslant 1$ pomerons exchanged between the vertex and the projectile hadron, $n \geqslant 1$ pomeron exchanges between the vertex and the target, subtracting the term with $m = n = 1$ (pomeron self-coupling), and integrating over rapidity $y_1 < Y = \ln\frac{s}{s_0}$ and impact parameter $\vec{b}_1$ of the vertex [9], see Fig. 2:

$$
\begin{aligned}
&\Delta\chi_{ad}^{\mathbb{PPP}}(s,b)\\
&\quad= \frac{G}{C_\pi^2}\sum_{m,n\geqslant 1;m+n\geqslant 3}\int_0^Y dy_1\\
&\qquad\times\int d^2b_1\frac{[-\chi_{a\pi}^{\mathbb{P}}(s_0e^{Y-y_1},|\vec{b}-\vec{b}_1|)]^m}{m!}\\
&\qquad\times\frac{[-\chi_{d\pi}^{\mathbb{P}}(s_0e^{y_1},b_1)]^n}{n!}\\
&\quad= \frac{G}{C_\pi^2}\int_0^Y dy_1\int d^2b_1\Big\{\big(1-e^{-\chi_{a\pi}^{\mathbb{P}}(s_0e^{Y-y_1},|\vec{b}-\vec{b}_1|)}\big)\\
&\qquad\times\big(1-e^{-\chi_{d\pi}^{\mathbb{P}}(s_0e^{y_1},b_1)}\big)\\
&\qquad-\chi_{a\pi}^{\mathbb{P}}\big(s_0e^{Y-y_1},|\vec{b}-\vec{b}_1|\big)\chi_{d\pi}^{\mathbb{P}}\big(s_0e^{y_1},b_1\big)\Big\}. \qquad (7)
\end{aligned}
$$

At $s\to\infty$ and $b, b_1 \to 0$ the integrand in the r.h.s. of (7) is dominated by the last term in the curly brackets, which corresponds to the contribution of the subtracted graph in Fig. 2. Thus, assuming that the main contribution to the integral over $\vec{b}_1$ in (7) comes from comparatively small b_1 and neglecting the slope of the multi-pomeron vertex, one obtains asymptotically

$$\Delta\chi_{ad}^{\text{asymp}(1)}(s,b) \sim -4\pi G\gamma_\pi^2\ln\frac{s}{s_0}\chi_{ad}^{\mathbb{P}}(s,b). \qquad (8)$$

Under the above assumptions the contributions of higher order graphs also reduce in the "dense" limit to subtracted pomeron self-couplings, which leads to [9]

$$\Delta\chi_{ad}^{\text{asymp}}(s,b) \sim \big((s/s_0)^{-4\pi G\gamma_\pi^2}-1\big)\chi_{ad}^{\mathbb{P}}(s,b). \qquad (9)$$

Thus, asymptotically one recovers the usual quasi-eikonal scheme based on re-normalized quasi-eikonal $\tilde{\chi}_{ad}^{\mathbb{P}} = \chi_{ad}^{\mathbb{P}} +$

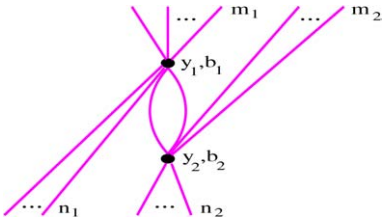

Fig. 3. An example of a "loop" graph.

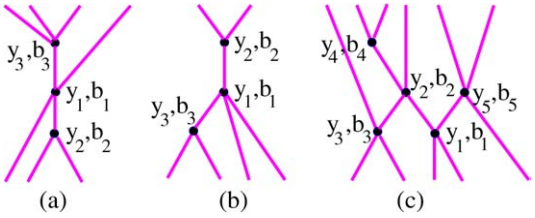

Fig. 4. Enhanced pomeron graphs of "tree" type (a,b) and of "net" type (c).

$\Delta\chi_{ad}^{\text{asymp}}$, which is defined by (4), (1), (2) with the pomeron intercept $\tilde{\alpha}_{\mathbb{P}}(0) = \alpha_{\mathbb{P}}(0) - 4\pi G\gamma_\pi^2$.

Our goal is to re-sum dominant enhanced diagrams to all orders, to obtain a smooth transition between the "dilute" (small energies, large impact parameters) and "dense" regimes. As in [9], we assume pion dominance of multi-pomeron vertices; treating $r_{3\mathbb{P}} = 4\pi GC_\pi\gamma_\pi^3$, $\gamma_{\mathbb{P}} = C_\pi\gamma_\pi$, $R_{\mathbb{P}}^2 = R_\pi^2$ as free parameters one may recover the general eikonal form for the pomeron vertices g_{mn} in case of proton–proton scattering.

We start from recalling that one can neglect contributions of "loop" graphs, which contain multi-pomeron vertices connected to each other by at least two pomerons, as shown in Fig. 3. Indeed, in the "dilute" regime such contributions are suppressed by powers of small triple pomeron coupling G (G^2 for the diagram of Fig. 3). On the other hand, in the "dense" limit, summing over any number n_1 of pomerons exchanged between the target and the upper vertex in Fig. 3 (similarly for the lower vertex), one obtains an exponential factor which strongly dumps the overall contribution [8,9]:

$$\sum_{n_1=0}^{\infty} \frac{[-\chi_{d\pi}^{\mathbb{P}}(s_0e^{y_1}, b_1)]^{n_1}}{n_1!} = e^{-\chi_{d\pi}^{\mathbb{P}}(s_0e^{y_1}, b_1)}. \tag{10}$$

Let us first re-sum contributions of "tree"-type graphs, shown in Fig. 4(a), (b). Those contain one "central" (not necessarily unique, see Fig. 4(b)) vertex, from which a number of pomeron "fans" develops towards the projectile and the target.

General "fan" contribution can be defined via the recursive equation of Fig. 5:

$$\begin{aligned}\chi_a^{\text{fan}}(y_1, b_1) &= \chi_{a\pi}^{\mathbb{P}}\big(s_0e^{y_1}, b_1\big) \\ &\quad + \frac{G}{C_\pi^2}\int_0^{y_1} dy_2 \int d^2b_2\, \chi_{\pi\pi}^{\mathbb{P}}\big(s_0e^{y_1-y_2}, |\vec{b}_1 - \vec{b}_2|\big) \\ &\quad \times \big[1 - e^{-\chi_a^{\text{fan}}(y_2,b_2)} - \chi_a^{\text{fan}}(y_2, b_2)\big].\end{aligned} \tag{11}$$

Thus, a general representation for "tree" graphs corresponds to the diagram with one "central" vertex connected to any number m of projectile "fans" χ_a^{fan} and to any number n of target

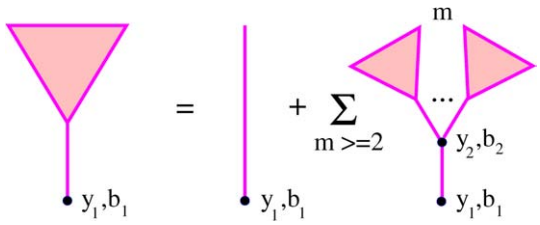

Fig. 5. Recursive equation for the "fan" contribution $\chi_a^{\text{fan}}(y_1, b_1)$; y_1 and b_1 are rapidity and impact parameter distances between hadron a and the vertex in the "handle" of the "fan".

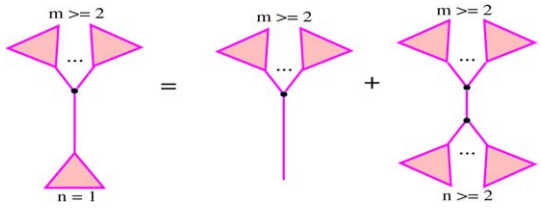

Fig. 6. "Tree" graphs with only one target "fan" can be expanded as shown in the figure.

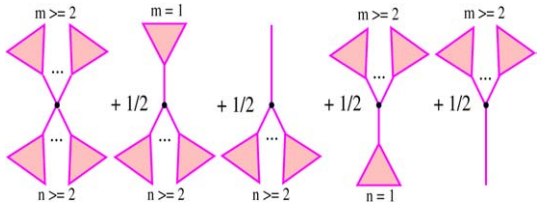

Fig. 7. Complete set of "tree" graphs.

ones χ_d^{fan}; $m, n \geqslant 1$, $m + n \geqslant 3$. However, here one should be careful with counting some contributions twice. For example, comparing the subsamples with $m = 2$, $n = 1$ and $m = 1$, $n = 2$, we can see that the graphs of the type of Fig. 4(b) are present in both cases. Let us consider the first case and express the lower (target) "fan" using the relation of Fig. 5, as shown in Fig. 6. A similar procedure can be performed in the second case ($m = 1$, $n = 2$), which results in the graphs of Fig. 6 being reversed upside-down, with the second diagram in the r.h.s. staying unchanged. Thus, correcting for such double counts, the overall "tree" type contribution is given by the set of graphs of Fig. 7, with

$$\begin{aligned}&\chi_{ad}^{\text{tree}}(s, b) \\ &\quad = \frac{G}{C_\pi^2}\int_0^Y dy_1 \int d^2b_1 \\ &\qquad \times \Big\{\big(1 - e^{-\chi_a^{\text{fan}}} - \chi_a^{\text{fan}}\big)\big(1 - e^{-\chi_d^{\text{fan}}} - \chi_d^{\text{fan}}\big) \\ &\qquad + \frac{1}{2}\big(\chi_a^{\text{fan}} + \chi_{a\pi}^{\mathbb{P}}\big)\big(1 - e^{-\chi_d^{\text{fan}}} - \chi_d^{\text{fan}}\big) \\ &\qquad + \frac{1}{2}\big(\chi_d^{\text{fan}} + \chi_{d\pi}^{\mathbb{P}}\big)\big(1 - e^{-\chi_a^{\text{fan}}} - \chi_a^{\text{fan}}\big)\Big\}.\end{aligned} \tag{12}$$

Here $\chi_{a\pi}^{\mathbb{P}} = \chi_{a\pi}^{\mathbb{P}}(s_0e^{Y-y_1}, |\vec{b} - \vec{b}_1|)$, $\chi_a^{\text{fan}} = \chi_a^{\text{fan}}(Y - y_1, |\vec{b} - \vec{b}_1|)$, $\chi_{d\pi}^{\mathbb{P}} = \chi_{d\pi}^{\mathbb{P}}(s_0e^{y_1}, b_1)$, $\chi_d^{\text{fan}} = \chi_d^{\text{fan}}(y_1, b_1)$.

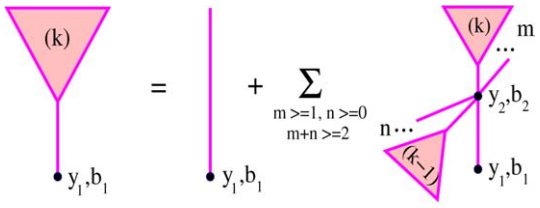

Fig. 8. Recursive equation for the "net fan" $\chi^{\mathrm{net}(k)}_{a|d}(y_1,\vec{b}_1|Y,\vec{b})$. The vertex (y_2,b_2) couples together m projectile "net fans" of kth order and n target "net fans" of $(k-1)$th order.

Let us come to more general diagrams of the type of Fig. 4(c), corresponding to arbitrary "nets" of pomerons. It is convenient to introduce some new building blocks. We define the "net fan" of kth order via the recursive equation of Fig. 8:

$$\begin{aligned}
&\chi^{\mathrm{net}(k)}_{a|d}(y_1,\vec{b}_1|Y,\vec{b})\\
&\quad=\chi^{\mathbb{P}}_{a\pi}\bigl(s_0e^{y_1},b_1\bigr)\\
&\qquad+\frac{G}{C_\pi^2}\int\limits_0^{y_1}dy_2\int d^2b_2\,\Bigl\{\Bigl[1-e^{-\chi^{\mathrm{net}(k)}_{a|d}(y_2,\vec{b}_2|Y,\vec{b})}\Bigr]\\
&\qquad\times\exp\bigl(-\chi^{\mathrm{net}(k-1)}_{d|a}\bigl(Y-y_2,\vec{b}-\vec{b}_2|Y,\vec{b}\bigr)\bigr)\\
&\qquad-\chi^{\mathrm{net}(k)}_{a|d}(y_2,\vec{b}_2|Y,\vec{b})\Bigr\}\chi^{\mathbb{P}}_{\pi\pi}\bigl(s_0e^{y_1-y_2},|\vec{b}_1-\vec{b}_2|\bigr).
\end{aligned}\tag{13}$$

Here we set

$$\chi^{\mathrm{net}(1)}_{a|d}(y_1,\vec{b}_1|Y,\vec{b})\equiv\chi^{\mathrm{fan}}_a(y_1,b_1),$$
$$\chi^{\mathrm{net}(0)}_{a|d}(y_1,\vec{b}_1|Y,\vec{b})\equiv 0.$$

By construction, the "net fan" of kth order contains contributions with a sequence of up to k pomerons connected to each other in a "zig-zag" way, such that pomeron end rapidities are arranged as $y_1>y_2<y_3>\cdots<y_k$. For example, the part of the graph of Fig. 4(c), positioned to the left of the vertex (y_1,b_1), can be considered as belonging to the projectile "net fan" of 3rd order; the "zig-zag" is formed by three pomerons: those exchanged between the vertices (y_1,b_1) and (y_2,b_2), (y_2,b_2) and (y_3,b_3), and by the leftmost pomeron connected to the projectile. Correspondingly, we define a "zig-zag fan" of kth order as the difference between kth and $(k-1)$th "net fans":

$$\chi^{\mathrm{zz}(k)}_{a|d}\equiv\chi^{\mathrm{net}(k)}_{a|d}-\chi^{\mathrm{net}(k-1)}_{a|d}.\tag{14}$$

Using the representation of Fig. 8 for the "net fan" contributions, $\chi^{\mathrm{zz}(k)}_{a|d}$ can be expressed as shown in Fig. 9. The two graphs in the r.h.s. of the figure differ by their uppermost vertices: in the 1st graph it couples together $m\geqslant 1$ projectile "net fans" of $(k-1)$th order, $q\geqslant 1$ target "zig-zag fans" of $(k-1)$th order and any number $n\geqslant 0$ of target "net fans" of $(k-2)$th order; the uppermost vertex of the 2nd graph is coupled to $p\geqslant 2$ projectile "zig-zag fans" of kth order and to any number $m\geqslant 0$ of projectile and $n\geqslant 0$ of target "net fans" of $(k-1)$th order. In addition, both graphs may contain any number $l\geqslant 0$ of intermediate vertices, coupled correspondingly to m_i projectile and n_i target "net fans" of $(k-1)$th order; $m_i,n_i\geqslant 0$, $m_i+n_i\geqslant 1$, $i=1,\ldots,l$.

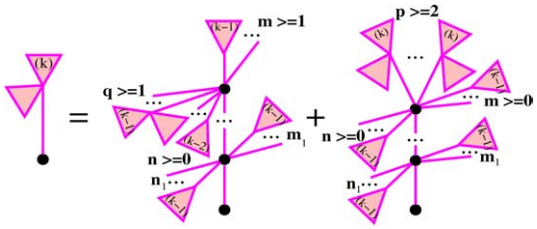

Fig. 9. "Zig-zag fan" $\chi^{\mathrm{zz}(k)}_{a|d}(y_1,\vec{b}_1|Y,\vec{b})$ can be represented as shown in the figure.

Now we can re-sum enhanced diagrams which contain "zig-zag fans" of kth order, starting from $k=2$, using the representation of Fig. 9 to correct for double counts in the same way as we did for "tree" graphs. This results in the set of diagrams of Fig. 10; the corresponding contribution to quasi-eikonal is

$$\begin{aligned}
&\chi^{\mathrm{enh}(k)}_{ad}(s,b)\\
&\quad=\frac{G}{C_\pi^2}\int\limits_0^Y dy_1\int d^2b_1\Bigl\{\bigl(1-e^{-\chi^{\mathrm{zz}(k)}_{a|d}}-\chi^{\mathrm{zz}(k)}_{a|d}\bigr)e^{-\chi^{\mathrm{net}(k-1)}_{a|d}}\\
&\qquad\times\bigl(1-e^{-\chi^{\mathrm{zz}(k)}_{d|a}}-\chi^{\mathrm{zz}(k)}_{d|a}\bigr)e^{-\chi^{\mathrm{net}(k-1)}_{d|a}}\\
&\qquad+\Bigl[\bigl(1-e^{-\chi^{\mathrm{zz}(k)}_{a|d}}-\chi^{\mathrm{zz}(k)}_{a|d}\bigr)e^{-\chi^{\mathrm{net}(k-1)}_{a|d}}\\
&\qquad\times\Bigl(1-e^{-\chi^{\mathrm{net}(k-1)}_{d|a}}+\frac{1}{2}\chi^{\mathrm{zz}(k)}_{d|a}e^{-\chi^{\mathrm{net}(k-1)}_{d|a}}\Bigr)\\
&\qquad+\frac{1}{2}\chi^{\mathrm{zz}(k)}_{a|d}\bigl(e^{-\chi^{\mathrm{zz}(k-1)}_{a|d}}-1\bigr)e^{-\chi^{\mathrm{net}(k-2)}_{a|d}}\\
&\qquad\times\bigl(1-e^{-\chi^{\mathrm{net}(k-1)}_{d|a}}\bigr)\Bigr]+[a\leftrightarrow d]\Bigr\}.
\end{aligned}\tag{15}$$

Here

$$\chi^{\mathrm{X}(k)}_{a|d}=\chi^{\mathrm{X}(k)}_{a|d}(Y-y_1,\vec{b}-\vec{b}_1|Y,\vec{b}),$$
$$\chi^{\mathrm{X}(k)}_{d|a}=\chi^{\mathrm{X}(k)}_{d|a}(y_1,\vec{b}_1|Y,\vec{b}),\qquad \mathrm{X}=\text{"zz"},\text{"net"}.$$

Finally, combining together the contributions $\chi^{\mathrm{tree}}_{ad}(s,b)$ and $\chi^{\mathrm{enh}(k)}_{ad}(s,b)$ for any $k\geqslant 2$ and using (13), (14), we can obtain for the full set of non-loop enhanced diagrams the representation of Fig. 11,with the eikonal contribution

$$\begin{aligned}
&\chi^{\mathrm{enh}}_{ad}(s,b)\\
&\quad=\chi^{\mathrm{tree}}_{ad}(s,b)+\sum_{k=2}^{\infty}\chi^{\mathrm{enh}(k)}_{ad}(s,b)\\
&\quad=\frac{G}{C_\pi^2}\int\limits_0^Y dy_1\int d^2b_1\Bigl\{\Bigl[\bigl(1-e^{-\chi^{\mathrm{net}}_{a|d}(1)}\bigr)\\
&\qquad\times\bigl(1-e^{-\chi^{\mathrm{net}}_{d|a}(1)}\bigr)-\chi^{\mathrm{net}}_{a|d}(1)\chi^{\mathrm{net}}_{d|a}(1)\Bigr]\\
&\qquad-\frac{G}{C_\pi^2}\int\limits_0^{y_1}dy_2\int d^2b_2\,\chi^{\mathbb{P}}_{\pi\pi}\bigl(s_0e^{y_1-y_2},|\vec{b}_1-\vec{b}_2|\bigr)\\
&\qquad\times\Bigl[\bigl(1-e^{-\chi^{\mathrm{net}}_{a|d}(1)}\bigr)e^{-\chi^{\mathrm{net}}_{d|a}(1)}-\chi^{\mathrm{net}}_{a|d}(1)\Bigr]\\
&\qquad\times\Bigl[\bigl(1-e^{-\chi^{\mathrm{net}}_{d|a}(2)}\bigr)e^{-\chi^{\mathrm{net}}_{a|d}(2)}-\chi^{\mathrm{net}}_{d|a}(2)\Bigr]\Bigr\}.
\end{aligned}\tag{16}$$

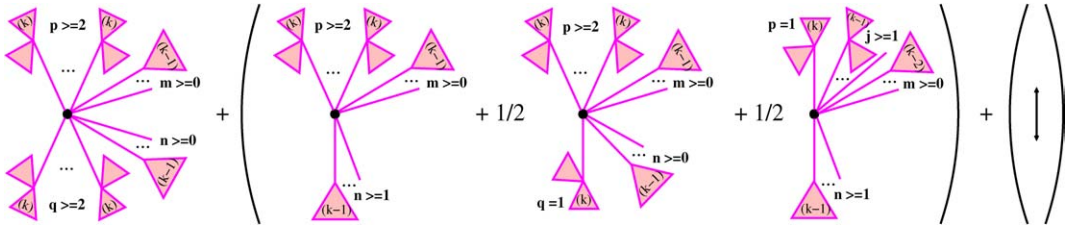

Fig. 10. Complete set of enhanced diagrams containing "zig-zag fans" of kth order.

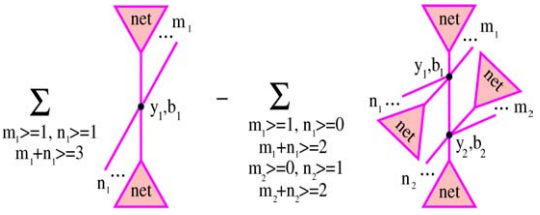

Fig. 11. Full set of non-loop diagrams.

Here we used the abbreviations $\chi^{\rm net}_{a|d}(i) = \chi^{\rm net}_{a|d}(Y - y_i, \vec{b} - \vec{b}_i|Y, \vec{b})$, $\chi^{\rm net}_{d|a}(i) = \chi^{\rm net}_{d|a}(y_i, \vec{b}_i|Y, \vec{b})$, $i = 1, 2$, and introduced general "net fan" contribution as $\chi^{\rm net}_{a|d} = \lim_{k\to\infty} \chi^{{\rm net}(k)}_{a|d}$. Using (13), we obtain for the latter the recursive equation

$$\begin{aligned}
&\chi^{\rm net}_{a|d}(y_1, \vec{b}_1|Y, \vec{b}) \\
&\quad = \chi^{\mathbb{P}}_{a\pi}\big(s_0 e^{y_1}, b_1\big) \\
&\qquad + \frac{G}{C_\pi^2}\int_0^{y_1} dy_2 \int d^2b_2 \big\{\big[1 - e^{-\chi^{\rm net}_{a|d}(y_2, \vec{b}_2|Y, \vec{b})}\big] \\
&\qquad \times \exp\big(-\chi^{\rm net}_{d|a}(Y - y_2, \vec{b} - \vec{b}_2|Y, \vec{b})\big) \\
&\qquad - \chi^{\rm net}_{a|d}(y_2, \vec{b}_2|Y, \vec{b})\big\} \chi^{\mathbb{P}}_{\pi\pi}\big(s_0 e^{y_1 - y_2}, |\vec{b}_1 - \vec{b}_2|\big). \qquad (17)
\end{aligned}$$

3. Numerical results

The obtained expressions allowed us to calculate hadronic elastic scattering amplitudes and correspondingly total cross sections and elastic scattering slopes with enhanced contributions taken into account. Here f_{ad}, $\sigma^{\rm tot}_{ad}$, $B^{\rm el}_{ad}$ are given by usual expressions (3)–(6), with the pomeron quasi-eikonal $\chi^{\mathbb{P}}_{ad}$ being replaced by $\chi^{\rm tot}_{ad} = \chi^{\mathbb{P}}_{ad} + \chi^{\rm enh}_{ad}$. Technically, the "net fan" contribution $\chi^{\rm net}_{a|d}$ has been obtained solving (17) iteratively and substituted to (16) to calculate enhanced diagram contribution $\chi^{\rm enh}_{ad}$. Concerning the parameter choice we used the usual values $C_p^2 = 1.5$, $C_\pi = 1.6/C_p$, $\gamma_\pi = 2/3\gamma_p$ [3], and from comparison to data obtained $\alpha_{\mathbb{P}}(0) = 1.18$, $\alpha'_{\mathbb{P}}(0) = 0.195$ GeV^{-2}, $\gamma_p = 1.59$ GeV^{-1}, $R_p^2 = 1.8$ GeV^{-2}, $R_\pi^2 = 0.7$ GeV^{-2}, $G_{3\mathbb{P}} = 9\times 10^{-3}$ GeV^2. Thus, for the triple-pomeron coupling we have $r_{3\mathbb{P}} = 4\pi G C_\pi \gamma_\pi^3 = 0.18$ GeV^{-1} compared to 0.12 GeV^{-1} and 0.083 GeV^{-1} in [9] and [10] correspondingly. The results for $\sigma^{\rm tot}_{pp}$, $\sigma^{\rm tot}_{\pi p}$, $B^{\rm el}_{pp}$ are shown in Fig. 12 as calculated with the full scheme or based on the bare pomeron eikonal $\chi^{\mathbb{P}}_{ad}$. In practice, it is sufficient to take into consideration only the "tree" $\chi^{\rm tree}_{ad}$ and the first "zig-zag" $\chi^{{\rm enh}(2)}_{ad}$ corrections, i.e. to use for the enhanced contribution $\tilde{\chi}^{\rm enh}_{ad} = \chi^{\rm tree}_{ad} + \chi^{{\rm enh}(2)}_{ad}$ instead of $\chi^{\rm enh}_{ad}$

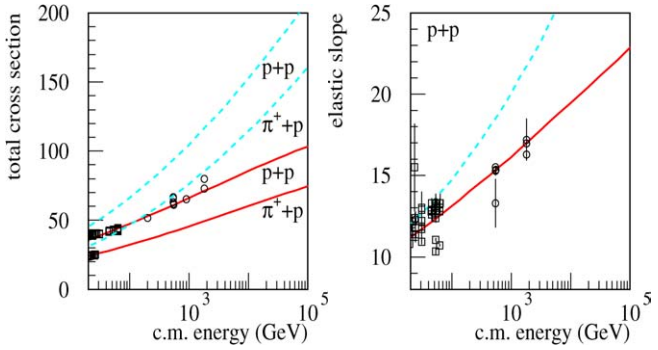

Fig. 12. Total cross section (left) and elastic scattering slope (right) as calculated with and without enhanced contributions—solid and dashed lines correspondingly. The compilation of data is from [12].

defined in (16); the difference for the calculated cross sections is below percent level. This is because the contributions $\chi^{{\rm enh}(k)}_{ad}$ for $k \geqslant 3$ are suppressed by exponential factors in the same way as for "loop" diagrams in (10).

Let us finally verify that the developed scheme approaches the asymptotic result (9) in the "dense" limit. Indeed, neglecting the radius of multi-pomeron vertices, at $s \to \infty$, $b \to 0$ and for $\alpha_{\mathbb{P}}(0) - 4\pi G\gamma_\pi^2 > 1$ we can obtain the solution of (17) as $\chi^{\rm net}_{a|d}(y_1, \vec{b}_1|Y, \vec{b}) \simeq \chi^{\mathbb{P}}_{a\pi}(s_0 e^{y_1}, b_1) + \Delta\chi^{\rm asymp}_{a\pi}(s_0 e^{y_1}, b_1)$, $\Delta\chi^{\rm asymp}_{a\pi}$ being defined in (9). Substituting this to (16), we see that the enhanced contribution $\chi^{\rm enh}_{ad}$ reduces to the asymptotic form (9): $\chi^{\rm enh}_{ad}(s, b) \simeq \Delta\chi^{\rm asymp}_{ad}(s, b)$.

In conclusion, we re-summed dominant enhanced contributions to elastic hadron–hadron scattering amplitude to all orders. Although the numerical calculations have been performed using the simple pomeron exchange amplitude (1), (2), the obtained formulas can be used for a different functional form of $f^{\mathbb{P}}_{ad}(s, b)$. In principle, one may apply similar techniques in the perturbative QCD, using the BFKL pomeron amplitude [13], provided eikonal approximation remains applicable for multi-pomeron vertices.

Acknowledgements

The author is indebted to R. Engel and A.B. Kaidalov for valuable discussions.

References

[1] V.N. Gribov, Sov. Phys. JETP 26 (1968) 414;
V.N. Gribov, Sov. Phys. JETP 29 (1969) 483.
[2] M. Baker, K.A. Ter-Martirosian, Phys. Rep. 28 (1976) 1;
A.B. Kaidalov, Phys. Rep. 50 (1979) 157.

[3] A.B. Kaidalov, K.A. Ter-Martirosyan, Phys. Lett. B 117 (1982) 247;
A. Capella, et al., Phys. Rep. 236 (1994) 225.
[4] V.A. Abramovskii, V.N. Gribov, O. Kancheli, Sov. J. Nucl. Phys. 18 (1974) 308.
[5] P. Aurenche, et al., Phys. Rev. D 45 (1992) 92;
K. Werner, Phys. Rep. 232 (1993) 87;
N. Kalmykov, S. Ostapchenko, Phys. At. Nucl. 56 (1993) 346.
[6] L. Gribov, E. Levin, M. Ryskin, Phys. Rep. 100 (1983) 1.
[7] O. Kancheli, JETP Lett. 18 (1973) 274;
A. Capella, J. Kaplan, J. Tran Thanh Van, Nucl. Phys. B 105 (1976) 333;
V.A. Abramovskii, JETP Lett. 23 (1976) 228.
[8] J.L. Cardi, Nucl. Phys. B 75 (1974) 413.
[9] A.B. Kaidalov, L.A. Ponomarev, K.A. Ter-Martirosyan, Sov. J. Nucl. Phys. 44 (1986) 468.
[10] S. Bondarenko, et al., Nucl. Phys. A 683 (2001) 649.
[11] S. Ostapchenko, in preparation.
[12] C. Caso, et al., Eur. Phys. J. C 3 (1998) 1.
[13] L.N. Lipatov, Sov. Phys. JETP 63 (1986) 904.